

The Efficacy and Environmental Implications of Engineered TiO₂ Nanoparticles in a Commercial Floor Coating

Yuqiang Bi[†], Tatiana Zaikova[□], Jared Schoepf[†], Pierre Herckes[§], James E. Hutchison[□]& and Paul
Westerhoff^{†*}

* Corresponding Author: p.westerhoff@asu.edu; 480-965-2885;

[†]School of Sustainable Engineering and the Built Environment, Arizona State University, Tempe, AZ 85287-3005

[□]Department of Chemistry and Biochemistry, University of Oregon, Eugene, OR 97403

[&]Materials Science Institute, University of Oregon, Eugene, OR 97403

[§]School of Molecular Sciences, Arizona State University, Tempe, AZ 85287-1604

In preparation for Submission to: *Environmental Science: Nano*

Date of Last Revision: August 15th, 2017

Table of contents

Table SI1. Standard conditions used for the Taber abrasion test on floor tiles, including the material of the abrasion wheels, the normal force, and the number of abrasive cycles (number of turntable revolutions).

Table SI2. Chemical composition of the commercial floor coating product determined by ICP-MS after HNO₃/HF microwave digestion.

Figure SI1. Fluorescent lamp irradiance spectrum from 300 to 800 nm for the antimicrobial efficacy test. UV light was found insignificant for this study.

Figure SI2. Transmission electron microscopy (TEM) micrographs of particles separated from the coating product with corresponding EDX results. (a) aggregates of TiO₂ nanoparticles; (b) amorphous potassium silicate; (c) histogram of TiO₂ particle size distribution.

Figure SI3. Wide-scan XPS spectrum collected from extracted solids from the commercial floor coating product.

Figure SI4. Scanning electron micrograph (SEM) of surface coated tile with the commercial product containing TiO₂ nanoparticles. The corresponding EDX result shows the dominance of silicon and potassium on the tile surfaces.

Figure SI5. SEM image of surface coated tile with the product containing additional food-grade TiO₂ nanoparticles for a surface coverage of ~10 mg/m². The corresponding EDX result shows clusters of TiO₂ nanoparticles on the tile surface after coating application.

Figure SI6. Optical profiler data showing the topography of coated tile surfaces with the original product (sample A) after the abrasion test using H-18 (coarse) abrasive. Surface roughness significantly increased after the abrasion, resulting in ~5 μm loss of surface thickness. The left side of the white bar shows the unabraded surface, and the right side shows the abraded surface.

Figure SI7. Water contact angle of coated floor samples with varied TiO₂ content. The inserted images above the bars illustrate the relative difference in contact angle during the measurement.

Figure SI8. Comparison of the first-order photocatalytic degradation of methyl orange (MO) in the presence of coating TiO₂, NIST SRM 1898, and food-grade TiO₂ under UV light irradiation at 312 nm. MO concentration was 10 mg/L, TiO₂ concentration was 60 mg/L, pH = 8.0.

Table S11. Standard conditions used for the Taber abrasion test on floor tiles, including the material of the abrasion wheels, the normal force, and the number of abrasive cycles (number of turntable revolutions).

Abrasion Wheel Type	Wheel Composition	Relative Abrasive Action	Wheel Weight	Number of cycles	Number of runs (replicates)
Wheel CS10	Rubber and aluminum oxide particles	Soft	1000 g	2500	5
Wheel H-18	Vitrified silica and aluminum oxide	Hard	500 g	100	5

Table SI2. Chemical composition of the commercial floor coating product determined by ICP-MS after HNO₃/HF microwave digestion.

Major Elements	Concentration in Original Product Sample A (mg/L)	wt.% in Original Product Sample A*	Concentration in Sample B Suspension (mg/L)
Potassium (K)	104,258 ± 3505	9.36	498.9 ± 28.1
Calcium (Ca)	31.1 ± 1.2	0.0028	175.7 ± 14.1
Sodium (Na)	285.4 ± 2.5	0.026	7.0 ± 1.8
Aluminum (Al)	41.8 ± 0.3	0.0038	10.9 ± 0.7
Iron (Fe)	35.5 ± 0.6	0.0032	21.1 ± 1.4
Titanium (Ti)	18.2 ± 0.8	0.0016	144.0 ± 10.5
Silicon (Si)	49,412 ± 513	4.44	2634.8 ± 210.8
Nickel (Ni)	0.2 ± 0.06	<0.001	< 0.3
Phosphorous (P)	30.7 ± 0.8	0.0028	3.5 ± 0.4
TiO ₂ solids	30.3 ± 1.3	0.003	242.4 ± 14.1

* The liquid coating product (sample A) has a density of ~1.11 kg/L.

Figure S11. Fluorescent lamp irradiance spectrum from 300 to 800 nm for the antimicrobial efficacy test. UV light was found insignificant for this study.

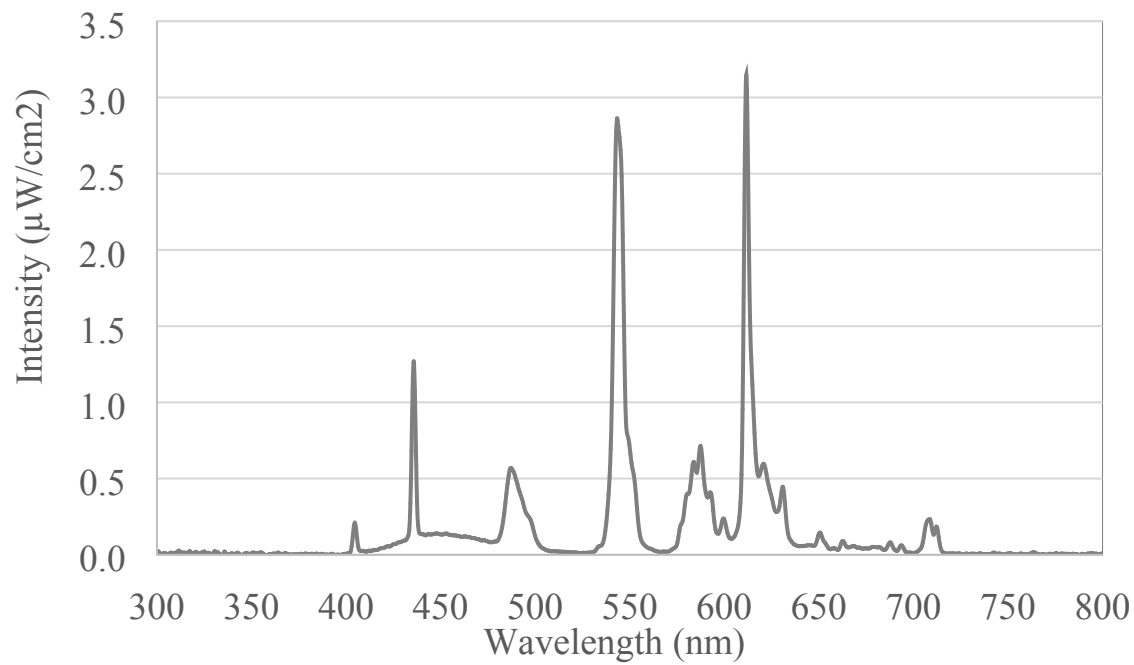


Figure S12. Transmission electron microscopy (TEM) micrographs of particles separated from the coating product with corresponding EDX results. (a) aggregates of TiO₂ nanoparticles; (b) amorphous potassium silicate; (c) histogram of TiO₂ particle size distribution.

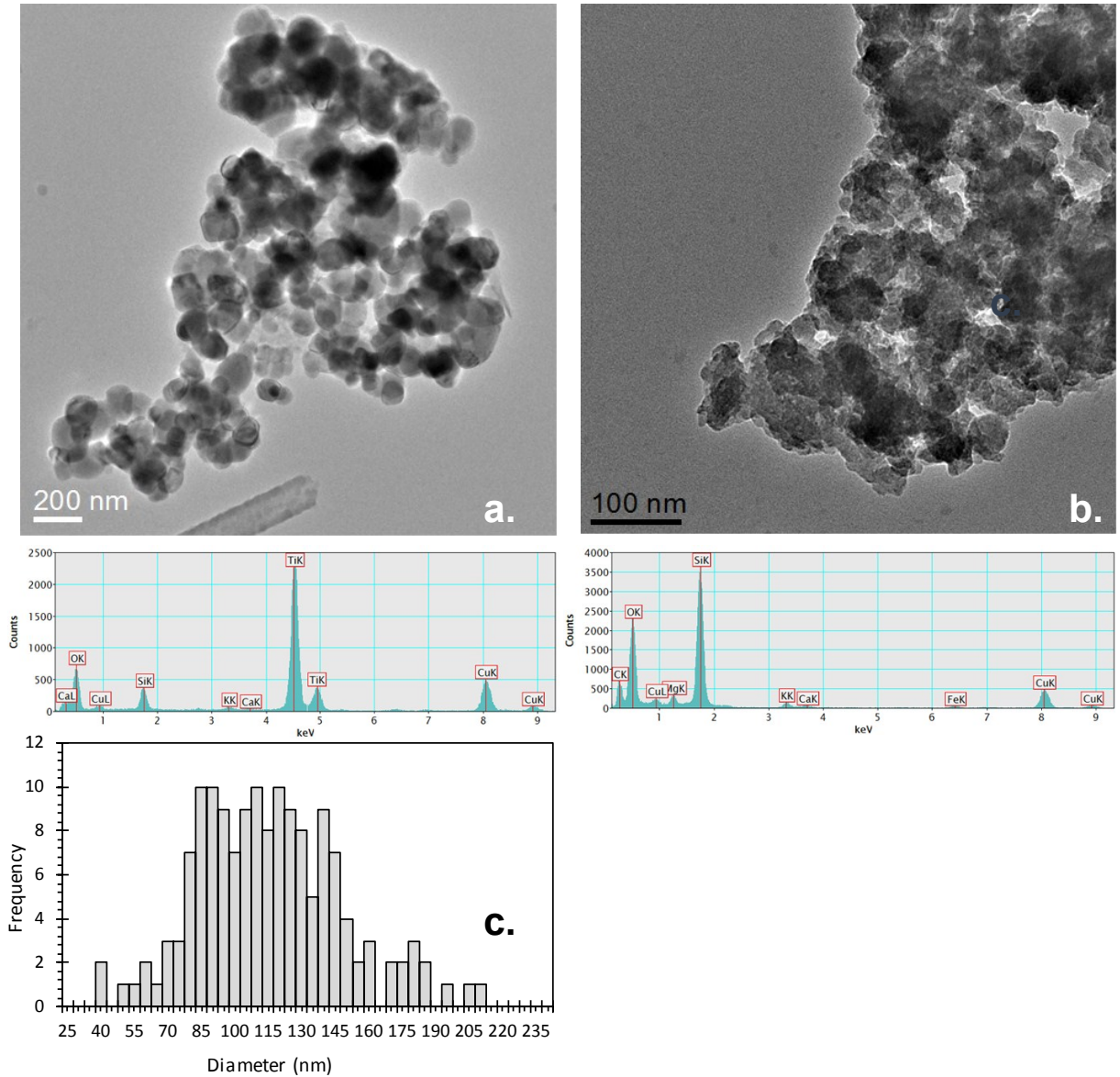


Figure S13. Wide-scan XPS spectrum collected from extracted solids from the commercial floor coating product.

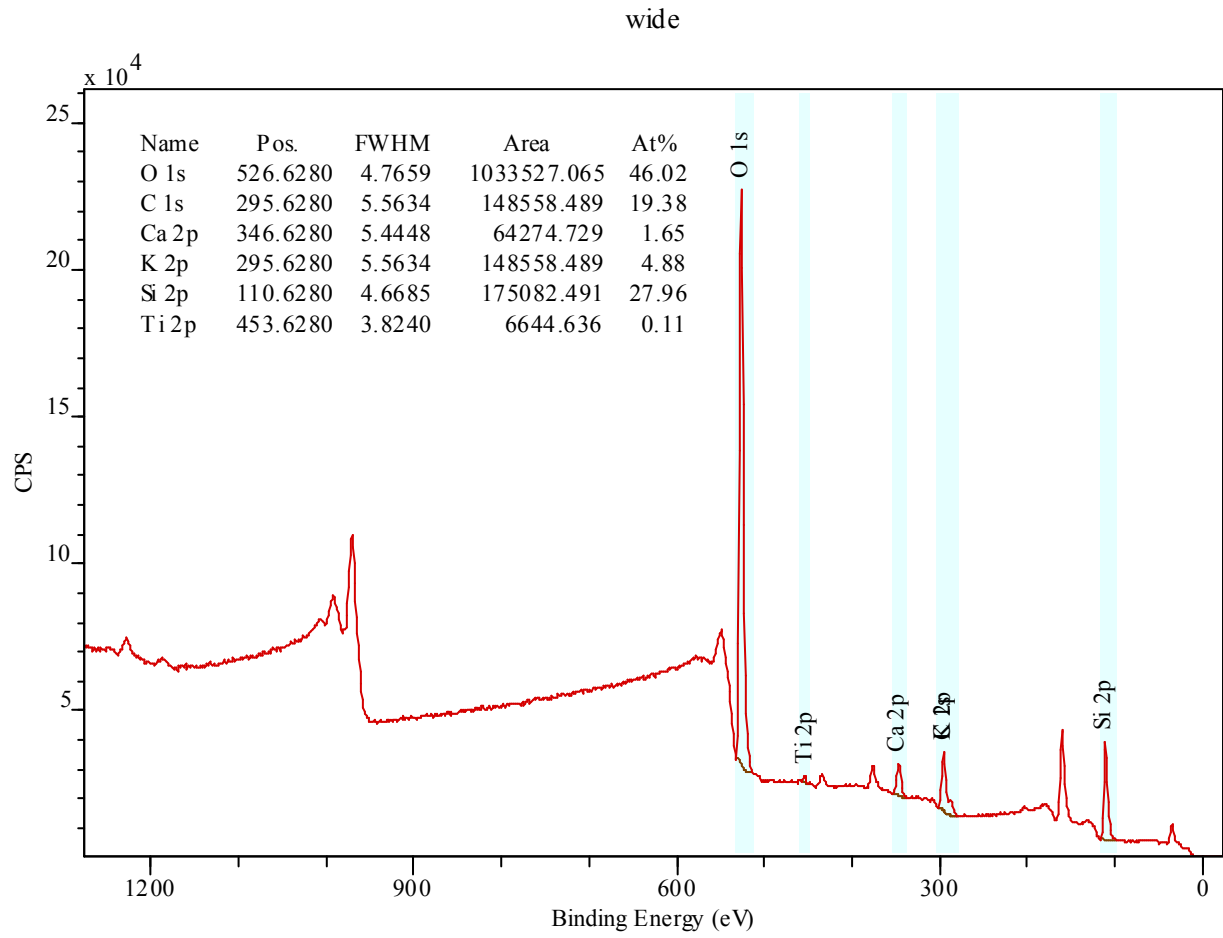


Figure SI4. Scanning electron micrograph (SEM) of surface coated tile with the commercial product containing TiO₂ nanoparticles. The corresponding EDX result shows the dominance of silicon and potassium on the tile surfaces.

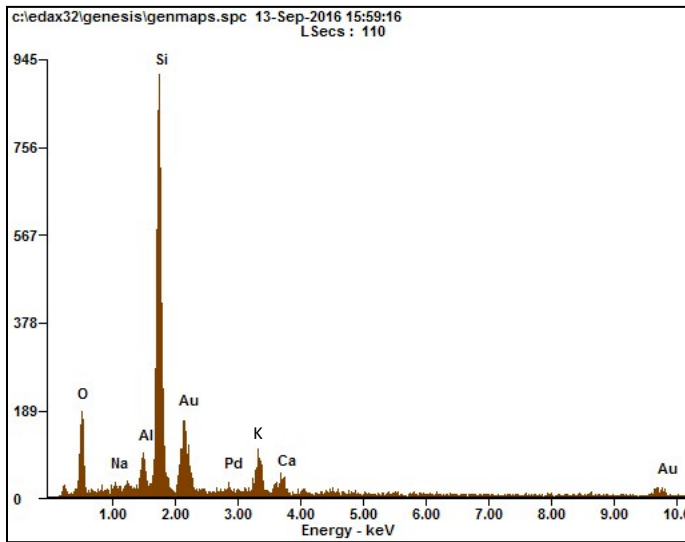
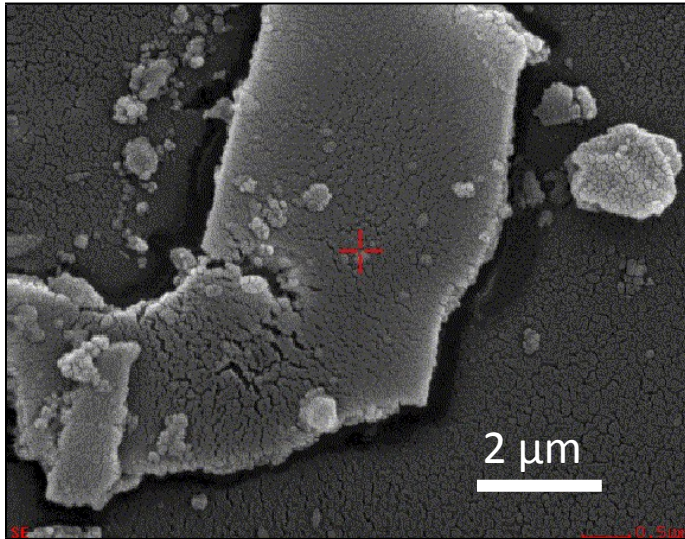


Figure S15. SEM image of surface coated tile with the product containing additional food-grade TiO_2 nanoparticles for a surface coverage of $\sim 10 \text{ mg/m}^2$. The corresponding EDX result shows clusters of TiO_2 nanoparticles on the tile surface after coating application.

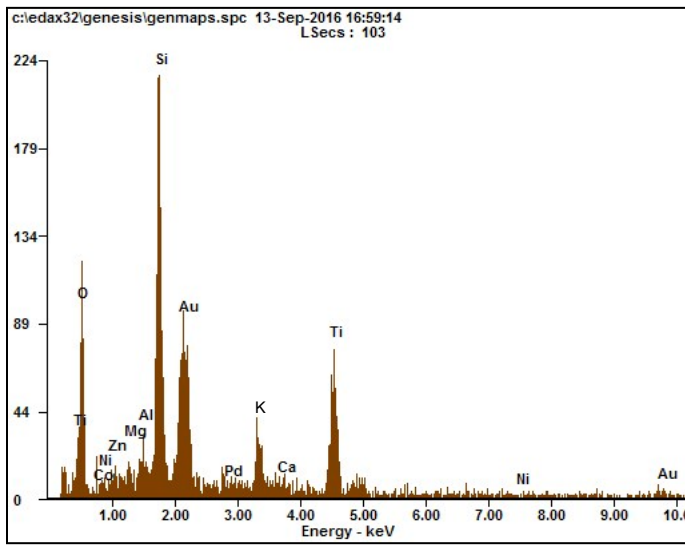
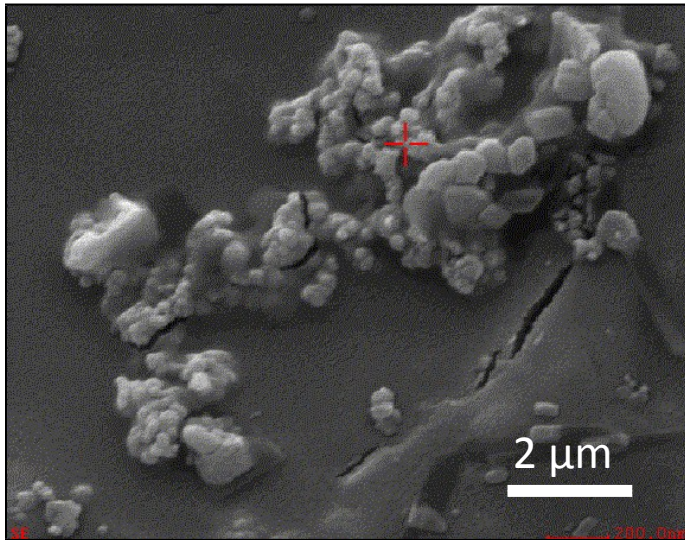


Figure SI6. Optical profiler data showing the topography of coated tile surfaces with the original product (sample A) after the abrasion test using H-18 (coarse) abrasive. Surface roughness significantly increased after the abrasion, resulting in $\sim 5 \mu\text{m}$ loss of surface thickness. The left side of the white bar shows the unabraded surface, and the right side shows the abraded surface.

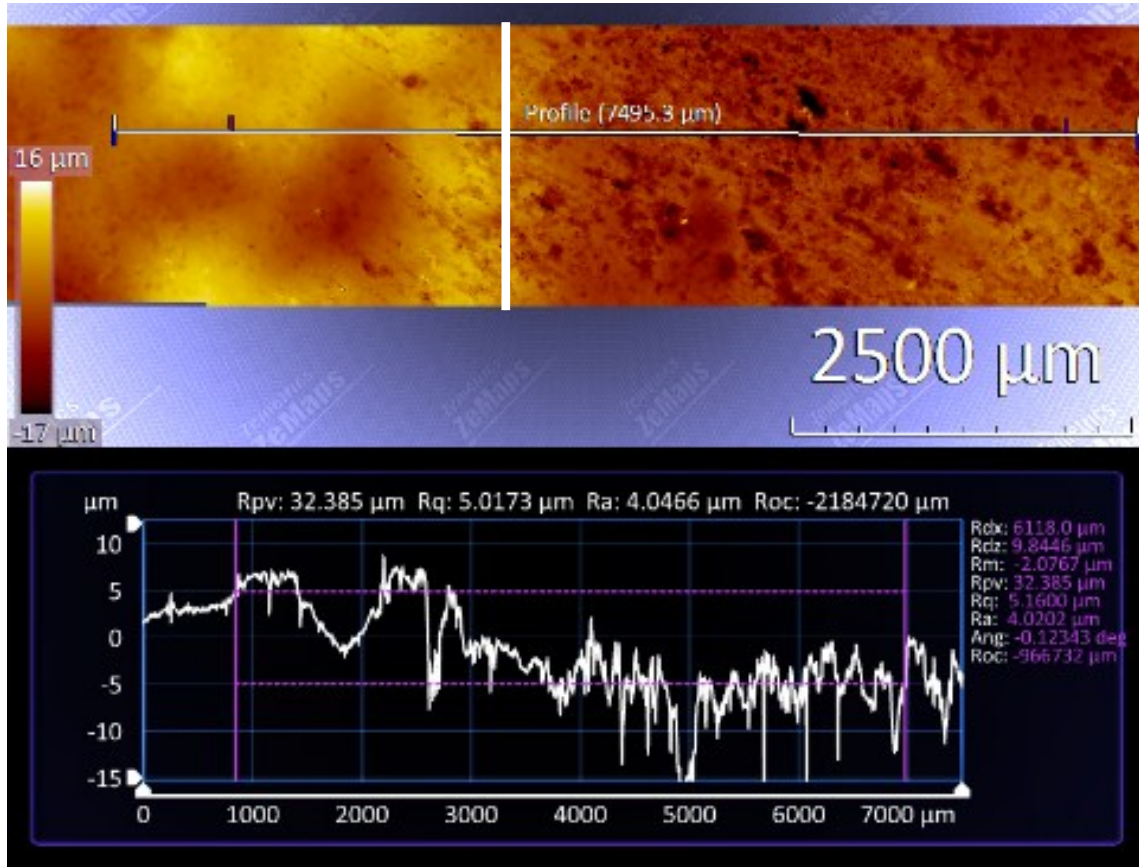


Figure S17. Water contact angle of coated floor samples with varied TiO_2 content. The inserted images above the bars illustrate the relative difference in contact angle during the measurement.

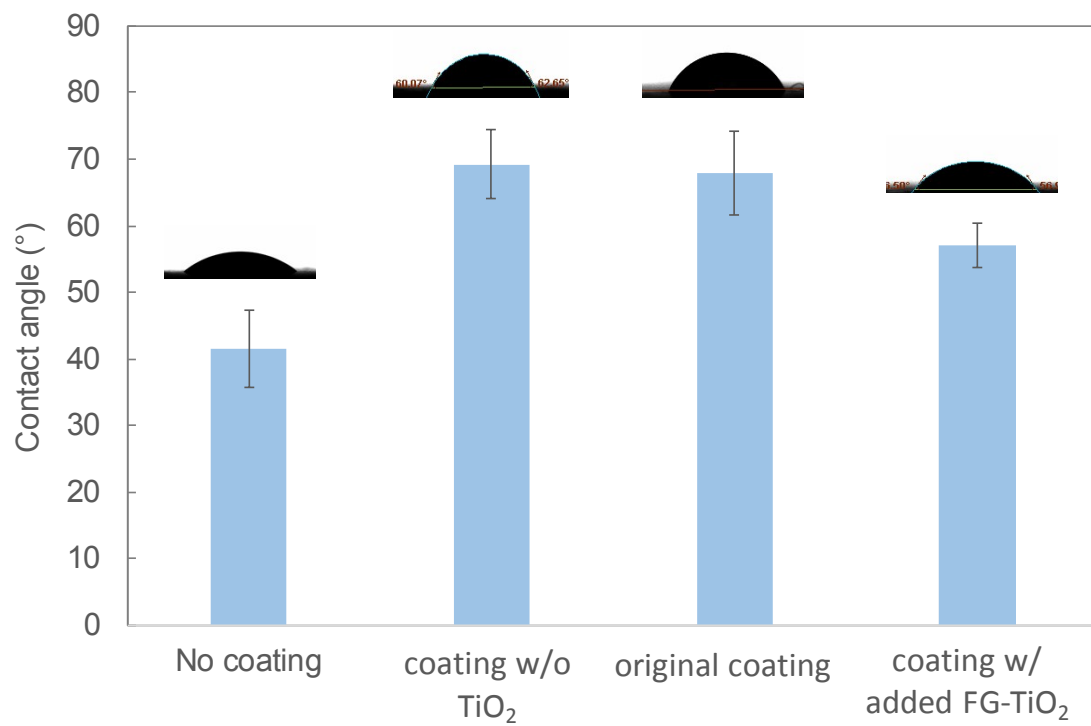


Figure SI8. Comparison of the first-order photocatalytic degradation of methyl orange (MO) in the presence of coating TiO₂, NIST SRM 1898, and food-grade TiO₂ under UV light irradiation at 312 nm. MO concentration was 10 mg/L, TiO₂ concentration was 60 mg/L, pH = 8.0.

